Can an ancillary ligand lead to a thermodynamically stable end-on 1 : 1 $Cu–O_2$ adduct supported by a β-diketiminate ligand?†

David E. Heppner, Benjamin F. Gherman, William B. Tolman and Christopher J. Cramer*

Received 26th June 2006, Accepted 16th August 2006
First published as an Advance Article on the web 25th August 2006
DOI: 10.1039/b608980a

The finding that dioxygen binds end-on to the Cu_B site in the crystal structure of a precatalytic complex of peptidylglycine α-hydroxylating monooxygenase has spurred the search for biomimetic model complexes exhibiting the same dioxygen coordination. Recent work has not only indicated that sterically hindered β-diketiminate ligands (L^1) could support side-on 1 : 1 $Cu–O_2$ adducts, but also that an end-on $L^1Cu(THF)O_2$ structure occurs as an unstable intermediate in the oxygenation mechanism of the Cu(I) complex. In this work, density functional theory and multireference methods are used to determine the potential of ancillary ligands, X, other than THF to yield thermodynamically stable end-on L^1CuXO_2 species. A diverse set of ligands X, comprising phosphines, thiophene, cyclic ethers, acetonitrile, *para*-substituted pyridines, N-heterocyclic carbenes, and ligands bearing hydrogen bond donors, has been considered in order to identify ligand characteristics which energetically favor end-on L^1CuXO_2 over: a) reversion to the Cu(I) complex and dioxygen, b) isomerization to side-on L^1CuXO_2, and c) decay to L^1CuO_2 and X. Ancillary ligands with judiciously chosen degrees and orientation of steric bulk and which bear potential hydrogen bond donors to an end-on bound dioxygen moiety most favor oxygenation of L^1CuX to yield end-on L^1CuXO_2. Conversion to the side-on isomer can be deterred through the use of a sufficiently bulky ligand X, such as one that is at least the size of a 5-membered ring. Loss of X to give L^1CuO_2 can be made prohibitively endergonic by employing ligands X which are highly electron donating and which backbond strongly with and σ-donate significantly to copper.

Introduction

Binding and activation of dioxygen at a monocopper site constitutes a fundamental reaction step in the catalytic cycles of numerous metalloenzymes.[1–3] Examples of two such systems are the neuroenzymes dopamine β-monooxygenase (DβM)[1,4] and peptidylglycine α-hydroxylating monooxygenase (PHM),[1,5] which catalyze the hydroxylation of the benzylic position of dopamine to yield norepinephrine and the hydroxylation of the C_α position of glycine-extended peptide precursors of neuropeptide hormones, respectively. DβM and PHM are believed to function by first forming a 1 : 1 $Cu–O_2$ adduct at their Cu_B sites (to which two histidine residues and one methionine residue are ligated *via* their side chains) and subsequently using this reactive intermediate species to hydroxylate the pertinent C–H bonds of their substrates.[6–8] A crystal structure of the copper–oxygen adduct in the PHM system obtained through the use of a bound, inactive substrate analog indicated η^1 (end-on) coordination of dioxygen to Cu_B.[9]

Recent years have seen significant efforts made in synthesizing and characterizing biomimetic 1 : 1 $Cu–O_2$ adducts as a means of furthering understanding of the formation and reactivity of these species in DβM and PHM.[10,11] Initial work in this area led to an η^2 (side-on) 1 : 1 $Cu–O_2$ complex supported by a sterically hindered tris(pyrazolyl)hydroborate ligand and illustrated that through the inclusion of sufficient steric bulk on the supporting ligand, 1 : 1 $Cu–O_2$ adducts could be isolated and reaction with a second Cu(I) to yield peroxodicopper or bis(μ-oxo)dicopper compounds could be inhibited.[12] Higher denticity tripodal tetradentate ligands, including tris(2-pyridylmethyl)amine (TPA or TMPA),[13,14] tris(2-pyridylethyl)amine (TEPA),[13] and tris(tetramethylguanidino)tren (TMG_3tren),[15,16] have been shown to be capable of supporting end-on 1 : 1 $Cu–O_2$ adducts based upon a combination of theoretical and experimental evidence. In addition, a copper(III)–hydroperoxide species which would otherwise be thermally unstable has been achieved using a tripodal pyridylamine ligand capable of donating hydrogen bonds to the HOO^- moiety.[17] A bisamide functionalized polyimidazole tripod ligand has also been shown to support a copper(II)–hydroperoxide stabilized by intramolecular hydrogen bonds to amide groups pendant from the imidazole rings.[18]

Other biomimetic modeling work has focused on the use of sterically hindered β-diketiminate and related ligands (Scheme 1),[19–24] which, like the Cu_B coordination environment in DβM and PHM,[25–30] contain only two nitrogen donors. In the case of the β-diketiminate ligand itself (L^1), an η^2 1 : 1 $Cu–O_2$ adduct was obtained and its structure and mechanism of formation extensively investigated through kinetic, spectroscopic, crystallographic, and theoretical techniques.[19–21] An asymmetric anilido–imine ligand (L^2), which differed from the β-diketiminate ligand by the presence of a phenyl ring fused to the ligand backbone, was also demonstrated to be capable of supporting an η^2 1 : 1 $Cu–O_2$ adduct,

Department of Chemistry and Supercomputer Institute, University of Minnesota, 207 Pleasant St. SE, Minneapolis, MN, 55455, USA

† Electronic supplementary information (ESI) available: Singlet–triplet free energy differences for all L^1CuXO_2 complexes and atomic coordinates for each computed geometry. See DOI: 10.1039/b608980a

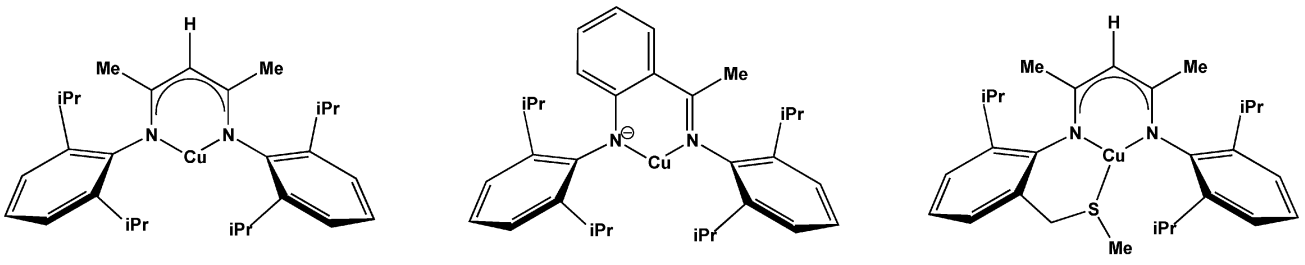

Scheme 1

which, despite the asymmetry of the ligand, proved to be virtually identical to that with L^1.[22] In an effort to better represent the two imidazole, one thioether coordination to Cu_B in DβM and PHM, a third ligand (L^3) was designed in which a thioether group was appended to one of the two flanking phenyl groups in L^1.[24] While the O_2 binding equilibrium is affected by the presence of the thioether functionality, an η^2 1 : 1 Cu–O_2 adduct is again obtained. Subsequent characterization of this complex showed that the structure of the adduct was not perturbed compared to that supported by L^1.[24] In short, despite the use of several different ligand systems, only side-on 1 : 1 Cu–O_2 adducts have been isolated, in contrast to the end-on dioxygen coordination seen in the crystal structure of the PHM precatalytic complex.[9] Furthermore, computations showed that η^1 structures supported by L^1, L^2, and L^3 were all thermodynamically unstable *versus* the η^2 isomers[21,22,24] and that the barrier for isomerization from η^1 to η^2 was minimal.[31]

However, within this body of work and specifically within the computed mechanism for oxygenation of the Cu(I)–THF complex with L^1,[21] there occurs an intriguing end-on bound dioxygen structure, $L^1Cu(THF)(O_2)$ (Fig. 1), which, while thermodynamically unstable, is a *bona fide* reaction intermediate. It has been proposed that coordination of THF to the copper center creates steric hindrance to simultaneous dioxygen coordination, leading to end-on dioxygen coordination and an elongated Cu–O bond length, factors which serve to destabilize this species *versus* the 1 : 1 adduct L^1CuO_2.[21]

The main question, therefore, to be investigated here is *whether an alternative ancillary ligand X could be employed instead of THF such that L^1CuXO_2 with end-on dioxygen coordination is thermodynamically stable with respect to reactants and energetically preferred* versus *either L^1CuXO_2 with side-on dioxygen coordination or the η^2-L^1CuO_2 1 : 1 adduct*. In other words, can a ligand X be identified which would satisfy the following three criteria (eqn (1)–(3)):

$$L^1CuX + O_2 \rightarrow \eta^1\text{-}L^1CuXO_2 \quad \Delta G_1 < 0 \tag{1}$$

$$\eta^1\text{-}L^1CuXO_2 \rightarrow \eta^2\text{-}L^1CuXO_2 \quad \Delta G_2 > 0 \tag{2}$$

$$\eta^1\text{-}L^1CuXO_2 \rightarrow X + \eta^2\text{-}L^1CuO_2 \quad \Delta G_3 > 0 \tag{3}$$

In order to answer this question, the oxygenation reaction of L^1CuX is examined here *via* theoretical calculations for a wide variety of ancillary ligands X (Scheme 2). Among the ligands that will be considered are cyclic ethers with varying degrees of steric bulk and ligands which strongly coordinate to Cu(I) such as pyridines and nitriles (*cf.* THF, which is weakly coordinating to Cu(I)). Ligands with varying electron donating capabilities will be explored, as more electron-rich ligands have been shown to lead to more exergonic free energies of oxygenation in computations on PHM active site models.[32] Given their resemblance to the methionine residue found at the Cu_B site in DβM[27–29,33] and PHM,[25,26,30] ligands containing a thioether functional group will likewise be surveyed. Finally, considering that the Cu_B site in PHM is exposed to the solvent-filled cleft between the two domains of the PHM protein[9,25,26,30] and that hydrogen-bonding interactions with water molecule(s) present may stabilize an end-on 1 : 1 Cu_B–O_2 adduct, ancillary ligands bearing hydrogen bond donors will be investigated.

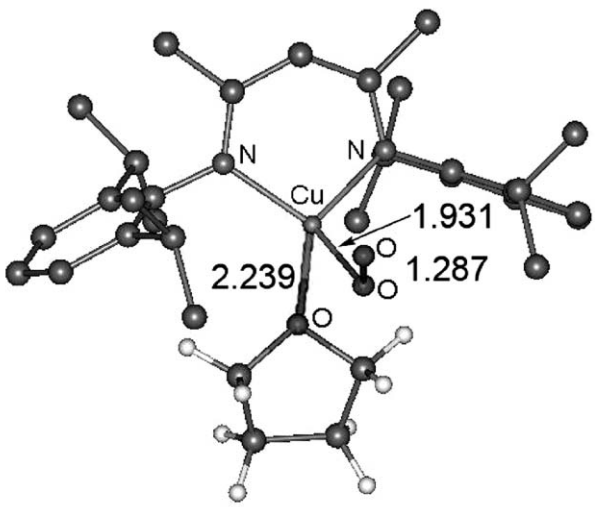

Fig. 1 $L^1Cu(THF)(O_2)$ intermediate exhibiting end-on dioxygen coordination from the oxygenation mechanism of $L^1Cu(THF)$.[21] Hydrogen atoms on L^1 are omitted for clarity. Distances are measured in Å. Unlabeled gray atoms are carbon; white atoms, H.

Computational methods

A. Density functional calculations

The Jaguar suite, version 5.0, of *ab initio* quantum chemistry programs was used for carrying out all geometry optimizations.[34] Having been shown to be successful in predicting ligand–Cu(I) and –Cu(II) bond dissociation energies,[35] density functional theory (DFT) with the B3LYP[36–38] functional was used in each of the

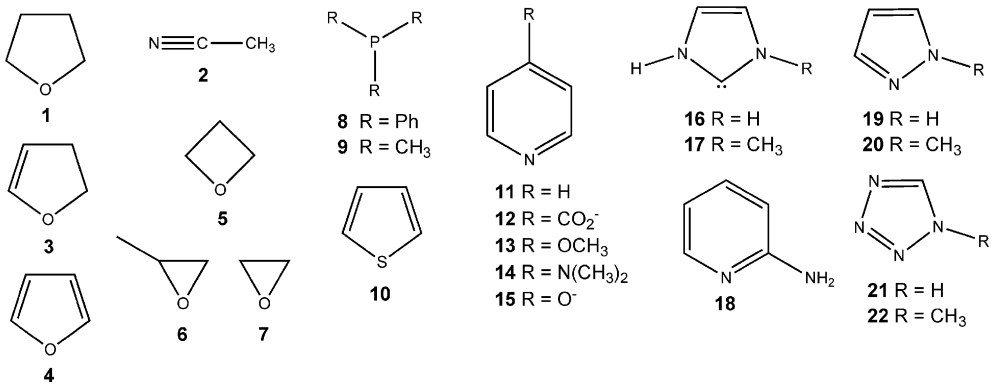

Scheme 2

calculations. Restricted (RDFT) and unrestricted (UDFT) levels of theory were applied in computations on singlet and triplet states, respectively, according to the established methodology for addressing complexes between Cu(I) and dioxygen.[21,22,24,31,32,39] The lacvp** effective core potential basis set[40–42] was used for Cu and the 6-31G** basis was used for all other atoms.

Mulliken charge populations are used to track electronic changes between the closely related structures that lie along the oxygenation pathway between L^1CuX and η^2-L^1CuO_2. These analyses, based upon DFT calculations in which balanced basis sets are used, have proven to be an effective means of tracking electron flow in a variety of systems involving the reaction of dioxygen at a metal center.[21,22,43,44]

Analytical vibrational frequency calculations were used to verify that optimized geometries were in fact stationary points. These calculations also allowed for zero-point energy, enthalpy, and entropic corrections, and hence free energies, to be determined. Truncated models were employed for these calculations in order to make them more tractable. The smaller models were obtained by replacing the four isopropyl groups on the flanking 2,6-diisopropyl groups of L^1 with hydrogen atoms and optimizing the positions of those hydrogen atoms while fixing the remainder of the structure.

For each optimized geometry, single-point solvation energies were calculated using the self-consistent reaction field method as implemented in the Poisson–Boltzmann solver in Jaguar.[45,46] In order to facilitate comparison to experimental data[21] and enhance relevance to potential future experimental work, the dielectric constant ε is taken to be that of THF (10.42 at −50 °C).[47,48] Computations of free energy changes in solution include a translational entropy correction to account for the change in concentration from gas phase (which, based upon a pressure of 1 atm, can be readily computed from the ideal gas law) to the 1 M standard-state solution concentration.[49] Despite the dielectric being set to that of THF, solvent THF is never considered here to be an explicit participant in chemical reactions. This avoids the need to account for solvent concentration in the entropy correction, which would erroneously stabilize L^1Cu(THF) compared to cases when other ancillary ligands are present.

B. Multireference calculations

Unlike closed-shell singlet and high-spin triplet Kohn–Sham wave functions which can be expressed as single Slater determinants, open-shell singlets require at minimum two determinants and thus are unable to be rigorously expressed within the framework of Kohn–Sham DFT. This consideration proves particularly relevant to computations on complexes between Cu(I) and dioxygen,[39] which may potentially possess significant Cu(II)–superoxo character, which in turn may be considered as resembling a biradical with one electron localized to Cu(II) and the other to O_2^-. Single-point multireference second-order perturbation theory (CASPT2) calculations[50] have been shown to be a reliable means of accounting for the multideterminantal nature of the singlet 1 : 1 Cu–O_2 adducts supported by L^1 and related ligands L^2 and L^3 and in active site models for DβM and PHM.[21,22,24,32]

Given the considerable inherent expense of CASPT2 computations, standard procedure has involved carrying out CASPT2 calculations only on a simplified version of L^1 in which both the backbone methyl groups and the 2,6-diisopropylphenyl flanking groups are changed to hydrogen atoms.[21,22,24,31] The difference in singlet–triplet energy splittings determined at the DFT and CASPT2 levels of theory is computed according to eqn (4).

$$\begin{aligned} \Delta &= ({}^1\mathrm{A} - {}^3\mathrm{A})_{\mathrm{CASPT2}} - ({}^1\mathrm{A} - {}^3\mathrm{A})_{\mathrm{DFT}} \\ &= [({}^1\mathrm{A})_{\mathrm{CASPT2}} - ({}^1\mathrm{A})_{\mathrm{DFT}}] - [({}^3\mathrm{A})_{\mathrm{CASPT2}} - ({}^3\mathrm{A})_{\mathrm{DFT}}] \end{aligned} \quad (4)$$

Given that triplet states are well described by DFT, the relative energy difference between the two levels of theory for the triplet state is taken to be zero. The quantity Δ, which is found to range from ~20 kcal mol^{-1} in the η^2-Cu–O_2 adducts to near 30 kcal mol^{-1} in the more superoxide-like η^1 cases, is then a measure of the relative energy difference for the singlet states between DFT and CASPT2 and can be utilized as a correction for the singlet energy provided by DFT. The final energies for singlet states are thus composed of the sum of the DFT energies from computations on the full L^1 systems and the Δ value for the corresponding simplified model. In a previous paper,[21] we demonstrated that for L^1 a linear correlation exists between Δ and the Cu–O bond length in the case of both side-on and end-on dioxygen coordination to the copper center. That result is used to facilitate the computation of Δ for the various copper–oxygen complexes examined herein.

In contrast to the application of DFT methods only, this procedure for combining results from DFT *and* CASPT2 calculations has been shown to yield singlet–triplet state orderings for the 1 : 1 Cu–O_2 adducts in these systems which are consistent with spectroscopic and crystallographic data.[21,22,24] This methodology has also proved successful in reproducing experimental kinetic

data for the oxygenation of $L^1Cu(MeCN)$, leading to theoretical predictions for enthalpies and free energies of activation within 1 kcal mol^{-1} of the experimental values.[21]

Results

A. Overview

Coordinative strengths of ancillary ligands X to Cu(I) ligated by L^1 relative to THF, as measured by determining ΔG for eqn (5) for each ligand X, are presented in Table 1.

$$L^1Cu(THF) + X \rightarrow L^1CuX + THF \quad (5)$$

Table 2 displays the free energies for oxygenating L^1CuX to yield the singlet η^2 1 : 1 adduct L^1CuO_2 (eqn (6)).

$$L^1CuX + O_2 \rightarrow L^1CuO_2 + X \quad (6)$$

Following this, the suitability of each ancillary ligand X for yielding a thermodynamically stable singlet η^1-L^1CuXO_2 complex is assessed through the determination of ΔG_1, ΔG_2, and ΔG_3 (eqn (1)–(3)) for each X (Table 3). Geometric and electronic changes upon oxygenation of the Cu(I) complexes to yield the singlet η^1-L^1CuXO_2 structures are enumerated in Tables 4 and 5, respectively. While triplet states have been calculated for all η^1-L^1CuXO_2 structures, they have nearly all been found to be higher in energy than their singlet counterparts by ~5–15 kcal mol^{-1} (Table S1†). The singlet–triplet splittings for the η^2-L^1CuXO_2 complexes either establish the singlet as the ground state or indicate the two states to be nearly isoenergetic (Table S1†). Consequently, only singlet states for the copper–oxygen complexes will be addressed in the following discussion.

We now turn to analyzing this body of data by comparing results within and between sets of related ligands X. This will enable an evaluation of the strengths and weaknesses of each ligand X with regard to stabilizing η^1-L^1CuXO_2 complexes. Lastly, these analyses will be pooled in order to derive the qualities that an ideal ligand X would have in order to yield a thermodynamically stable η^1-L^1CuXO_2 geometry.

Table 1 Relative coordinative strengths of ligands X to Cu(I) *versus* THF, as measured by the free energy change for the ligand substitution reaction: $L^1Cu(THF) + X \rightarrow L^1CuX + THF$

X	ΔG/kcal mol^{-1}
THF (**1**)	0.0
MeCN (**2**)	−5.2
2,3-Dihydrofuran (**3**)	0.8
Furan (**4**)	4.5
Oxetane (**5**)	−0.9
Methyloxirane (**6**)	2.9
Oxirane (**7**)	0.5
Triphenylphosphine (**8**)	−0.7
Trimethylphosphine (**9**)	−4.8
Thiophene (**10**)	2.9
Pyridine (**11**)	−7.7
4-Pyridinecarboxylate (**12**)	−3.9
4-Methoxypyridine (**13**)	−6.4
N,*N*-Dimethyl-4-pyridinamine (**14**)	−8.4
4-Oxypyridine (**15**)	−11.9
Carbene (**16**)	−24.6
Methylcarbene (**17**)	−25.1
2-Pyridinamine (**18**)	−5.8
Pyrazole (**19**)	−8.4
1-Methylpyrazole (**20**)	−5.8
Tetrazole (**21**)	−2.1
N-Methyltetrazole (**22**)	0.6

Table 2 Free energies of oxygenation for the L^1CuX complexes for all ligands X to generate η^2-L^1CuO_2 (*i.e.*, ΔG for the reaction: $L^1CuX + O_2 \rightarrow \eta^2$-$L^1CuO_2 + X$)

X	ΔG/kcal mol^{-1}
THF (**1**)	−14.4
MeCN (**2**)	−9.3
2,3-Dihydrofuran (**3**)	−15.2
Furan (**4**)	−18.9
Oxetane (**5**)	−13.6
Methyloxirane (**6**)	−17.4
Oxirane (**7**)	−15.0
Triphenylphosphine (**8**)	−13.8
Trimethylphosphine (**9**)	−4.8
Thiophene (**10**)	−17.4
Pyridine (**11**)	−6.8
4-Pyridinecarboxylate (**12**)	−10.6
4-Methoxypyridine (**13**)	−8.1
N,*N*-Dimethyl-4-pyridinamine (**14**)	−6.0
4-Oxypyridine (**15**)	−2.6
Carbene (**16**)	10.1
Methylcarbene (**17**)	10.7
2-Pyridinamine (**18**)	−8.6
Pyrazole (**19**)	−6.1
1-Methylpyrazole (**20**)	−8.7
Tetrazole (**21**)	−12.3
N-Methyltetrazole (**22**)	−15.1

B. Phosphines

In the cases of both triphenylphosphine (**8**) and trimethylphosphine (**9**), oxygenating L^1CuX to form η^1-L^1CuXO_2 is energetically unfavorable, as evidenced by positive values for ΔG_1. The steric bulk of the phosphines inhibits strong Cu–O_2 interactions. The proximal Cu–O distances of 2.11 Å and 2.03 Å in $L^1Cu(\mathbf{8})O_2$ and $L^1Cu(\mathbf{9})O_2$, respectively, are notably longer than the average of ~1.95 Å in the other η^1–L^1CuXO_2 complexes. Steric bulk from the phosphines likewise prevents η^2-L^1CuXO_2 geometries from being stable under optimization. The exergonic ΔG_3 values are consistent with dioxygen binding to Cu(I) being energetically preferred over either triphenylphosphine or trimethylphosphine coordination. Displacement of THF by O_2 in $L^1Cu(THF)$ to yield η^2-L^1CuO_2 is more energetically favorable than displacement of THF by **8** or **9** to yield $L^1Cu(\mathbf{8})$ or $L^1Cu(\mathbf{9})$ by 13.7 kcal mol^{-1} and 9.6 kcal mol^{-1}. In brief, the phosphine ancillary ligands, with positive ΔG_1 and negative ΔG_3 values, are unfavorable with respect to yielding thermodynamically stable η^1-L^1CuXO_2 species.

The energies for displacement of THF by dioxygen and triphenylphosphine also lead to the prediction that $\Delta G = +13.7$ kcal mol^{-1} at 223 K for the reaction in eqn (7)

$$L^1CuO_2 + \mathbf{8} \rightarrow L^1Cu(\mathbf{8}) + O_2 \quad (7)$$

when all species are assumed to be at their standard state concentrations. This reaction was only observed to occur experimentally, though, upon warming from 193 K to room temperature,[23] at which the computed ΔG changes to +8.4 kcal mol^{-1}. By comparison, oxygenation of $L^1Cu(MeCN)$ is reported to be nonreversible and ΔG for O_2 displacement by MeCN is computed to be +8.9 kcal mol^{-1}.[21] The discrepancy between the different observed reactivities and nearly equal ΔG values for dioxygen displacement

Table 3 Assessment of the criteria for ligands X stabilizing an η^1-L^1CuXO_2 complex, as measured by the free energy changes ΔG_1, ΔG_2, and ΔG_3 for eqn (1)–(3)

X	ΔG_1/kcal mol^{-1}	ΔG_2/kcal mol^{-1}	ΔG_3/kcal mol^{-1}
THF (**1**)	−2.4	>0[a]	−12.0
MeCN (**2**)	7.3	>0[b]	−16.6
2,3-Dihydrofuran (**3**)	1.4	>0[a]	−16.6
Furan (**4**)	0.1	>0[a]	−19.0
Oxetane (**5**)	0.1	−4.6	−13.7
Methyloxirane (**6**)	−2.1	−4.8	−15.3
Oxirane (**7**)	−0.6	−4.6	−14.3
Triphenylphosphine (**8**)	4.2	>0[a]	−17.9
Trimethylphosphine (**9**)	4.2	>0[a]	−9.0
Thiophene (**10**)	3.1	>0[a]	−20.5
Pyridine (**11**)	3.4	2.0	−10.2
4-Pyridinecarboxylate (**12**)	−2.1	9.2	−8.5
4-Methoxypyridine (**13**)	−0.6	7.3	−7.5
N,*N*-Dimethyl-4-pyridinamine (**14**)	0.6	9.5	−6.6
4-Oxypyridine (**15**)	1.6	8.0	−4.2
Carbene (**16**)	−1.5	8.4	11.6
Methylcarbene (**17**)	5.3	5.6	5.4
2-Pyridinamine (**18**)	3.7	5.3	−12.4
Pyrazole (**19**)	0.6	7.6	−6.8
1-Methylpyrazole (**20**)	2.8	6.5	−11.5
Tetrazole (**21**)	−5.2	>0[a]	−7.1
N-Methyltetrazole (**22**)	2.6	>0[a]	−17.7

[a] No stable geometry for η^2-L^1CuXO_2 could be obtained in these cases, indicating this reaction is prohibitively uphill. [b] No stable geometry for η^2-L^1CuXO_2 could be obtained in this case. The η^1-L^1CuXO_2 intermediate proceeds through an unstable geometry identifiable as an η^2-L^1CuXO_2 structure to give L^1CuO_2 + X in a barrierless fashion.[21]

Table 4 Geometric changes upon oxygenation of L^1CuX to yield η^1-L^1CuXO_2

X	Δ(Cu–X)/Å	Δ(O–O)[a]/Å
THF (**1**)	0.165	0.072
MeCN (**2**)	0.685	0.067
2,3-Dihydrofuran (**3**)	0.138	0.067
Furan (**4**)	0.403	0.072
Oxetane (**5**)	0.137	0.073
Methyloxirane (**6**)	0.536	0.067
Oxirane (**7**)	0.133	0.080
Triphenylphosphine (**8**)	−0.024	0.057
Trimethylphosphine (**9**)	0.063	0.065
Thiophene (**10**)	0.330	0.071
Pyridine (**11**)	0.142	0.066
4-Pyridinecarboxylate (**12**)	0.043	0.061
4-Methoxypyridine (**13**)	0.083	0.065
N,*N*-Dimethyl-4-pyridinamine (**14**)	0.073	0.064
4-Oxypyridine (**15**)	0.015	0.064
Carbene (**16**)	0.077	0.092
Methylcarbene (**17**)	0.053	0.075
2-Pyridinamine (**18**)	0.203	0.081
Pyrazole (**19**)	0.167	0.091
1-Methylpyrazole (**20**)	0.073	0.063
Tetrazole (**21**)	0.217	0.102
N-Methyltetrazole (**22**)	0.595	0.067

[a] Measured *versus* the calculated equilibrium triplet dioxygen bond length of 1.215 Å.

Table 5 Changes in Mulliken charge population upon oxygenation of L^1CuX to yield η^1-L^1CuXO_2

X	$\Delta(L^1Cu)$	ΔX	ΔO_2
THF (**1**)	0.43	−0.01	−0.42
MeCN (**2**)	0.44	0.00	−0.44
2,3-Dihydrofuran (**3**)	0.43	−0.02	−0.41
Furan (**4**)	0.48	−0.05	−0.43
Oxetane (**5**)	0.48	−0.04	−0.44
Methyloxirane (**6**)	0.49	−0.05	−0.44
Oxirane (**7**)	0.44	0.02	−0.46
Triphenylphosphine (**8**)	0.30	0.04	−0.34
Trimethylphosphine (**9**)	0.31	0.05	−0.36
Thiophene (**10**)	0.41	−0.01	−0.40
Pyridine (**11**)	0.40	0.02	−0.42
4-Pyridinecarboxylate (**12**)	0.38	0.01	−0.39
4-Methoxypyridine (**13**)	0.40	0.01	−0.41
N,*N*-Dimethyl-4-pyridinamine (**14**)	0.36	0.05	−0.41
4-Oxypyridine (**15**)	0.36	0.05	−0.41
Carbene (**16**)	0.51	0.00	−0.51
Methylcarbene (**17**)	0.33	0.08	−0.41
2-Pyridinamine (**18**)	0.52	−0.05	−0.47
Pyrazole (**19**)	0.56	−0.06	−0.50
1-Methylpyrazole (**20**)	0.36	0.02	−0.38
Tetrazole (**21**)	0.58	−0.02	−0.56
N-Methyltetrazole (**22**)	0.44	−0.01	−0.43

can be attributed to problems with the applied level of theory accurately describing Cu-**8** interactions in L^1Cu(**8**), leading in turn to an underestimation of the stability of L^1Cu(**8**). When the polarized triple-ζ 6-311G* basis set is applied to phosphorous, the reaction in eqn (7) is predicted to have an exergonic ΔG of −5.1 kcal mol^{-1}, in agreement with the experimentally observed reactivity.[23] The necessity for the larger basis set here is apparently singular to the phosphine cases. Previous computations addressing dioxygen reactivity with L^1Cu(MeCN), L^1Cu(THF), L^2Cu(MeCN), and L^3Cu led to thermodynamic, kinetic, and geometric results which accorded well with experimental results.[21,22,24,31] The theoretical challenge in modeling the Cu–P bond is illustrated by the optimized geometry for L^1Cu(**8**), which shows a Cu–P bond length 0.14 Å longer than that observed in the crystal structure (2.32 Å, computed; 2.18 Å crystal).[23] This difference is singularly longer than the 0.05 Å maximum differences obtained between

computed geometries and all other available crystal structures with the L^1 and L^2 systems,[51] in particular those for $L^1Cu(MeCN)$ and L^1CuO_2,[21] $L^2Cu(MeCN)$ and L^2CuO_2,[22] and $L^1Cu(\mathbf{16})$ (*vide infra*).[52]

C. Thiophene

With thiophene (**10**) as the ancillary ligand X to the β-diketiminate ligand with its two nitrogen donors, greater resemblance to the N_2S coordination found at the Cu_B site in DβM[27–29,33] and PHM[25,26,30] is achieved. However, thiophene did not lead to a thermodynamically stable η^1-L^1CuXO_2 complex. The size of the thiophene ligand disfavored dioxygen binding to give η^1-$L^1Cu(\mathbf{10})O_2$. The endergonicity of ΔG_1 originated in part as well from disruption of the Cu(I)–S ligation as the copper center is oxidized and the Cu–S distance increases by 0.33 Å from that in $L^1Cu(\mathbf{10})$. A similar increase in Cu–S distance was seen upon oxygenation of L^3Cu[24] and with oxidation of the Cu_B site in DβM.[28] A stable η^2-$L^1Cu(\mathbf{10})O_2$ geometry could not be obtained. As in the L^3 case,[24] conversion from η^1-$L^1Cu(\mathbf{10})O_2$ to η^2-dioxygen coordination is exergonic ($\Delta G_3 = -20.5$ kcal mol^{-1}) and is accompanied by complete loss of the Cu–S ligation.

D. Cyclic ethers

Comparing the cyclic ethers with five-membered rings (THF (**1**), 2,3-dihydrofuran (**3**), and furan (**4**)), $LCu(\mathbf{3})$ has the highest ΔG_1 (Table 3). The essentially planar ring of 2,3-dihydrofuran is tilted in η^1-$L^1Cu(\mathbf{3})O_2$ such that one hydrogen atom of the CH_2 group proximal to copper sterically impacts on the dioxygen moiety (Fig. 2). $LCu(\mathbf{4})$ is intermediate with respect to ΔG_1 for oxygenation. With no sp^3 carbons, furan has no hydrogen atoms extending out of the plane of the cyclic ether, which minimizes steric influence on O_2 binding to copper. However, furan, unlike THF and 2,3-dihydrofuran (*cf*. Table 5), functions as an electron withdrawing group upon formation of η^1-$L^1Cu(\mathbf{4})O_2$ by absorbing 0.05 e.u. of electron density into π* orbitals associated with the carbon–carbon double bonds in the furan ring. The lowest ΔG_1 occurs for the case of THF. The pucker in the THF ring results in the two CH_2 groups in THF proximal to copper being positioned away from the site of dioxygen binding. This leads to an increase of 0.10 Å in the closest contact of a hydrogen atom from THF with dioxygen, compared to that with 2,3-dihydrofuran and furan. Among the smaller cyclic ethers, ΔG_1 decreases in going from oxetane (**5**), to oxirane (**7**), to methyloxirane (**6**). Oxetane bears to two CH_2 groups which provide steric hindrance to O_2 coordination. Oxirane is a smaller ring structure than oxetane, but like oxetane still presents two CH_2 groups worth of steric bulk near the copper center. Steric hindrance is minimized in methyloxirane, where one set of out-of-plane hydrogen atoms is located one C–C bond length farther from the copper center as compared to oxirane. The smaller size of these cyclic ethers allows for closer Cu–O_2 interactions in η^1-L^1CuXO_2 as compared to the larger cyclic ethers and consequently greater reduction of O_2, by 0.02–0.05 e.u., in η^1-L^1CuXO_2 (Table 5). Stable η^2-L^1CuXO_2 geometries were obtained only for the cases of the smaller cyclic ethers, which presented relatively less steric bulk around the copper center. The large exergonic ΔG_3 values in all cases are consistent with the loss of the weakly coordinating cyclic ethers to yield L^1CuO_2.

In summary, the greatest thermodynamic preference for η^1-L^1CuXO_2 over $L^1CuX + O_2$ occurs with THF and methyloxirane and use of the larger cyclic ethers can inhibit conversion to η^2-L^1CuXO_2. However, in none of these cases is η^1-L^1CuXO_2 stable with respect to decay to $L^1CuO_2 + X$.

E. Acetonitrile

The high ΔG_1 (+7.3 kcal mol^{-1}) in the case of acetonitrile (**2**) can be related to the similarity of η^1-$L^1Cu(\mathbf{2})O_2$ and the transition state for the bimolecular reaction of $L^1Cu(\mathbf{2}) + O_2$.[21] In fact, the two structures differ in energy by only 2.0 kcal mol^{-1}.

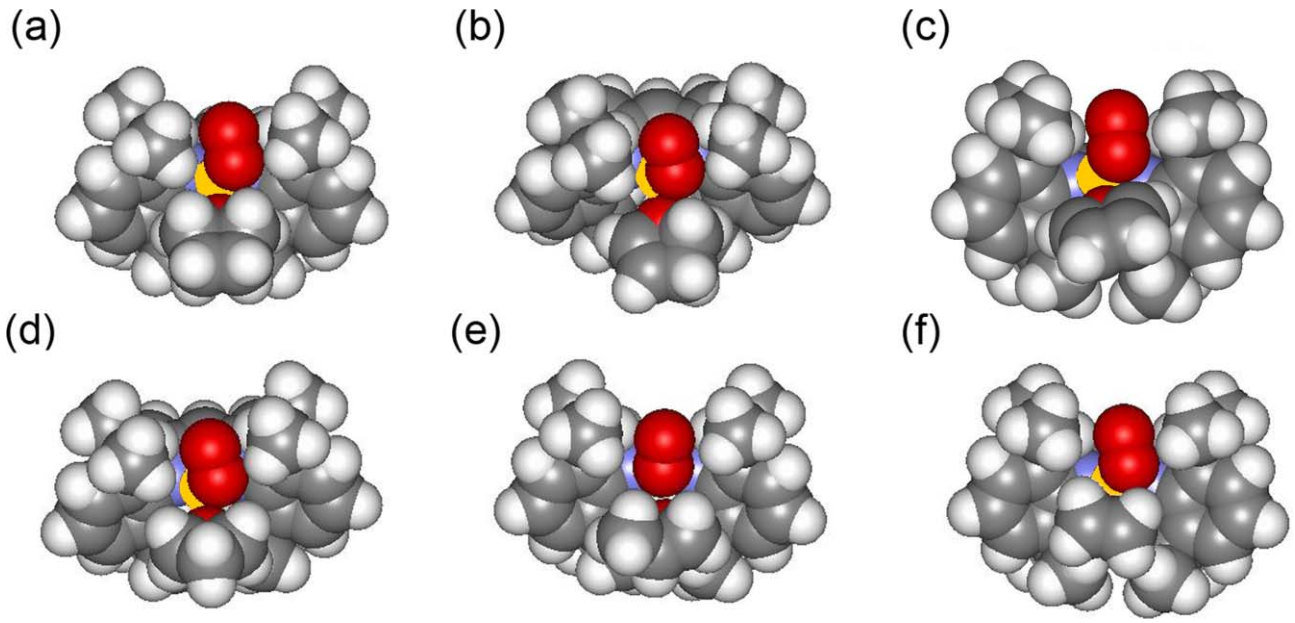

Fig. 2 Space-filling representations of the end-on L^1CuXO_2 complexes, where X is (a) THF, (b) 2,3-dihydrofuran, (c) furan, (d) oxetane, (e) methyloxirane, and (f) oxirane of the cyclic ether series. Yellow stands for Cu; gray, C; blue, N; red, O; white, H.

The η^1-L^{1}Cu(**2**)O_2 complex exhibits a long Cu–**2** bond length of 2.62 Å and an increase in Cu–**2** bond length *versus* that in L^{1}Cu(**2**) of 0.685 Å. A lower energy η^2-L^{1}Cu(**2**)O_2 geometry can be identified, but it is not a minima on the potential energy surface.[21] Formation of L^{1}CuO_2 from η^1-L^{1}Cu(**2**)O_2 is predicted to be exergonic, confirming that acetonitrile is not suitable for generating a thermodynamically stable η^1-L^{1}CuXO_2 species.

F. *para*-Substituted pyridines

Comparing ΔG for L^{1}CuO_2 formation from L^{1}CuX + O_2 where X is a *para*-substituted pyridine reveals competing effects (Table 2). More strongly coordinating or electron-rich ligands raise ΔG by stabilizing L^{1}CuX, but also lead to lowering ΔG as the solvation energies of X increase. The net result is a decrease in ΔG as electron-donating character increases in going from pyridine (**11**) to 4-pyridinecarboxylate (**12**), followed by progressively higher free energy changes with 4-methoxypyridine (**13**), *N*,*N*-dimethyl-4-pyridinamine (**14**), and 4-oxypyridine (**15**) as the Cu(I)–X bond strength becomes the dominant factor.

Among the pyridine ancillary ligands, pyridine itself has the most endergonic ΔG_1 and the largest increase in Cu–X bond length upon oxygenation of L^{1}CuX to give η^1-L^{1}CuXO_2. The Δ(Cu–X) of 0.142 Å is about 0.07 Å more than with the substituted pyridines (Table 4), likely due to these ligands being more electron rich and coordinating more strongly to the copper center. A negative Hammett correlation between σ_p[53] and ΔG_1 exists for the substituted pyridines **12–15** (Fig. 3a). As the substituted pyridines become increasingly electron rich, they also become increasingly

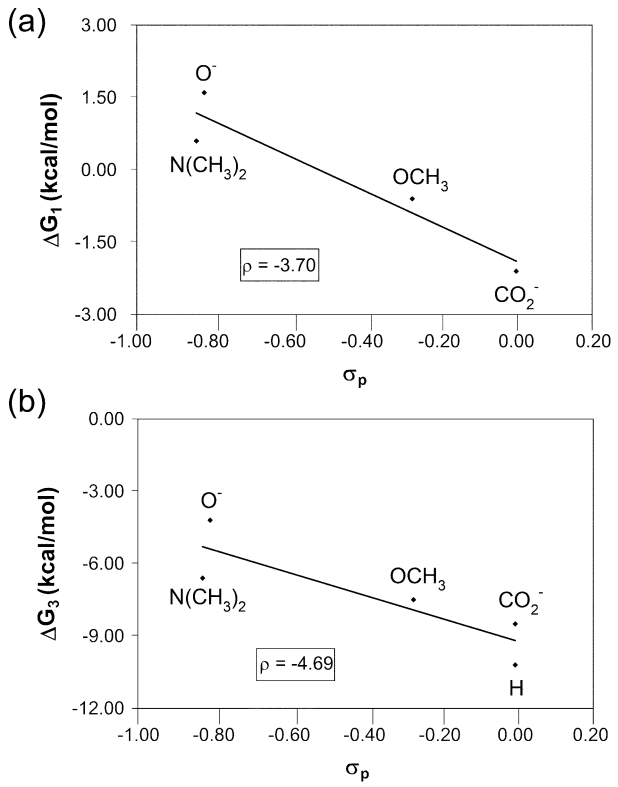

Fig. 3 Correlation of the Hammett substituent constants (σ_p) with the (a) ΔG_1 and (b) ΔG_3 values for the *para*-substituted (–N(CH$_3$)$_2$, –O$^-$, –OCH$_3$, –CO$_2^-$, –H) pyridine series of ligands X.

strongly coordinated to Cu(I) (*cf.* Table 1). Binding dioxygen to the L^{1}CuX complexes weakens this Cu–X ligation, which leads to increasing values for ΔG_1 as the electron-donating character of X increases. Conversion to η^2-L^{1}CuXO_2 from η^1-L^{1}CuXO_2 is nearly equally energetically uphill for each of the substituted pyridines due to a uniformly large amount of steric bulk in each case disfavoring a five-coordinate copper center. All ΔG_3 values are negative but do become less exergonic as the electron-donating character of the substituted pyridine increases, as evidenced by the negative Hammett correlation for ΔG_3 (Fig. 3b). This is turn can be connected with the relative electron-donating capabilities of the substituted pyridines and the corresponding degrees to which they stabilize the η^1-L^{1}CuXO_2 species.

With comparable ΔG_1 values to those of the cyclic ether series but less exergonic ΔG_3 values (by ~8 kcal mol^{-1} on average), the substituted pyridines better stabilize η^1-L^{1}CuXO_2 structures than the cyclic ethers. Neither of these two classes of ancillary ligands, however, yield thermodynamically stable η^1-L^{1}CuXO_2 intermediates.

G. N-Heterocyclic carbenes

Two different N-heterocyclic carbenes have been considered here: 2,3-dihydro-1*H*-imidazol-2-ylidene (hereafter, denoted "carbene" (**16**)) and methyl-2,3-dihydro-1*H*-imidazol-2-ylidene (hereafter, denoted "methylcarbene" (**17**)). The former bears N–H groups which can serve as hydrogen bond donors, while the latter methyl-substituted carbene more accurately reflects products which may be obtained *via* experimental synthesis.[54] The Cu–C bond lengths in L^{1}Cu(**16**) and L^{1}Cu(**17**) of 1.944 Å and 1.958 Å are consistent with the corresponding bond length of 1.918 Å in a recently reported crystal structure of a Cu(I) complex supported by a less sterically hindered β-diketiminate ligand with 1,3-dimesityl-2,3-dihydro-1*H*-imidazol-2-ylidene.[52]

The carbenes rank nearly equally as the most strongly coordinating ligands X to L^{1}Cu (*cf.* Table 1).[55] In particular, the coordinative strength of carbene is 12.7 kcal mol^{-1} greater than 4-oxypyridine, the next strongest coordinating ligand to L^{1}Cu, and 16.9 kcal mol^{-1} greater than pyridine. This difference can be attributed to the ability of carbene to act particularly strongly as both a σ-donor and π-acceptor in its coordination to the metal center.[56] NBO perturbation theory[57,58] indicates that σ-donation from the carbon lone pair of the carbene stabilizes L^{1}Cu(**16**) significantly more than the corresponding interaction in L^{1}Cu(**11**). π-backbonding between the Cu(I) center and the empty p_z orbital of the carbene is also predicted to generate 7.4 kcal mol^{-1} more stabilization compared to back-donation from copper into the π* orbitals of the pyridine ring.

Comparing ΔG_1 for the two carbene cases, η^1-L^{1}Cu(**16**)O_2 formation (Fig. 4a) is seen to be slightly exergonic ($\Delta G_1 = -1.5$ kcal mol^{-1}), and also 6.8 kcal mol^{-1} lower than for η^1-L^{1}Cu(**17**)O_2 where no hydrogen bond between the carbene and the oxygen atom of O_2 distal to the copper center is formed. The hydrogen bond in η^1-L^{1}Cu(**16**)O_2 leads to greater reduction of dioxygen by 0.10 e.u. and a 0.018 Å longer O–O bond length in this case *versus* η^1-L^{1}Cu(**17**)O_2. The moderate size of the carbene rings does not prohibit formation of η^2-L^{1}CuXO_2 geometries, but does make isomerization from η^1-L^{1}CuXO_2 energetically unfavorable. Finally, the very strong carbene–copper interaction makes severing this

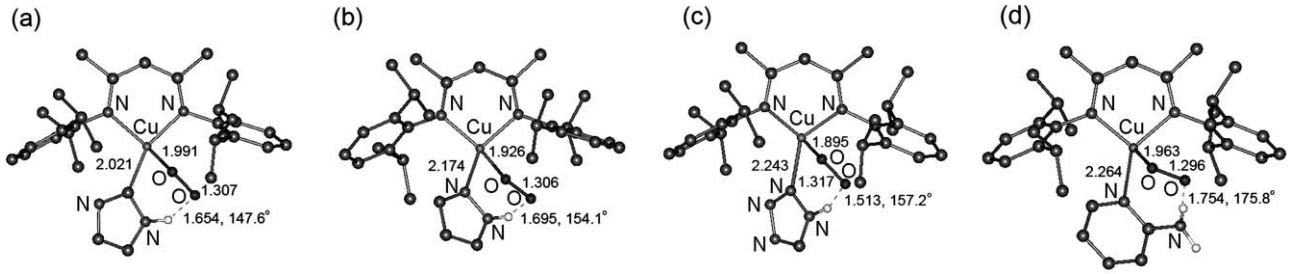

Fig. 4 End-on L^1CuXO_2 complexes, where X is (a) carbene, (b) pyrazole, (c) tetrazole, and (d) 2-pyridinamine. Dashed lines represent hydrogen bonds. Hydrogen atoms not involved in hydrogen bonding are omitted for clarity. Distances are measured in Å. Angles correspond to ∠N–H–O of the hydrogen bond. Unlabeled gray atoms are carbon; white atoms, H.

ligation to yield L^1CuO_2 + X an endergonic process. Among the various ancillary ligands X considered in this study, the carbene ligands are the only cases to yield $\Delta G_3 > 0$, which coincides with the carbenes being the only ligands X to coordinate more strongly to copper than dioxygen. Taken together, these results show that the carbene ancillary ligand (**16**) is uniquely capable among the ligands examined in this study of yielding a thermodynamically stable η^1-L^1CuXO_2 species.

H. Hydrogen bond donor ligands

As the carbene ligand with N–H groups cannot be synthesized,[54] various other ligands bearing hydrogen bond donors are next considered. Such hydrogen bonding may play a role in stabilizing Cu_B–O_2 adducts in PHM given that the Cu_B site sits adjacent to the water-filled cleft that separates the two copper centers in PHM.[9,25,26] Intramolecular hydrogen bonding has also been used as a design strategy in other biomimetic models for DβM and PHM,[18,59] copper superoxide dismutase model systems,[60] manganese(III)–peroxo complexes,[61] and metal ion mediated activation of dioxygen in general.[62]

Comparing pyrazole (**19**) and 1-methylpyrazole (**20**), close structural analogs for the carbene and methylcarbene ancillary ligands, reveals that hydrogen bonding between pyrazole and the dioxygen moiety lowers ΔG_1 by 2.2 kcal mol^{-1} (Fig. 4b). The weaker coordination of the pyrazole ligands to copper nonetheless renders η^1-L^1CuXO_2 unstable with respect to decay to L^1CuO_2 + X in these cases. Tetrazole (**21**) and *N*-methyltetrazole (**22**) are next considered as more electron-rich analogs of pyrazole and 1-methylpyrazole. As with the carbene and pyrazole ligands, hydrogen bonding between tetrazole and the O_2 group (Fig. 4c) leads to a lowering of ΔG_1 (here by 7.8 kcal mol^{-1}) *versus* the *N*-methyltetrazole case. The tetrazoles are rather weakly coordinating to L^1Cu (*cf.* Table 1), and the ΔG_3 are correspondingly exergonic. Use of 2-pyridinamine (**18**) as the ligand X, notably, does not lead to a more stable η^1-L^1CuXO_2 as compared to the case of pyridine. Despite the formation of a hydrogen bond in η^1-L^1Cu(**18**)O_2 (Fig. 4d), ΔG_1 for the 2-pyridinamine case is 0.3 kcal mol^{-1} higher than with pyridine. Lastly, geometry optimizations confirmed that the $-NH_2$ group in 3-pyridinamine is located too far from the copper center to capably act as a hydrogen bond donor to copper-bound dioxygen.

The 6-membered chelate rings that result from hydrogen bond formation between dioxygen and ancillary ligands lead to decreases in ΔG_1 of 2–8 kcal mol^{-1}. On the other hand, the 7-membered chelate ring that forms as a result of the hydrogen bonding in η^1-L^1Cu(**18**)O_2 is not as energetically preferred as the 6-membered chelate rings which form in the cases of carbene, pyrazole, and tetrazole. Competing effects of stabilization due to the hydrogen bond and geometric strain combine to leave ΔG_1 virtually unchanged between the pyridine and 2-pyridinamine cases.

I. Implications for biomimetic modeling

Examination of the successes and failures of the various ancillary ligands X in leading to a thermodynamically stable η^1-L^1CuXO_2 species reveals several characteristics that an ideal ligand X would possess. The ease of oxygenating L^1CuX to yield η^1-L^1CuXO_2 (as measured by ΔG_1) can be enhanced by careful modification of steric effects in the immediate vicinity of the Cu–O_2 unit, as illustrated in the case of the cyclic ether ligands. The size and orientation of the ancillary ligand when bound to L^1Cu as well as the amount of steric bulk immediately adjacent to the ligating atom of the ligand X all effect the ΔG_1 value. Inclusion of hydrogen bond donors on ligands X such that 6- rather than 7-membered chelate rings are formed in η^1-L^1CuXO_2 can also serve to lower ΔG_1 (*cf.* 2-pyridinamine *versus* other hydrogen-bond donor ligands). Isomerization from η^1- to η^2-L^1CuXO_2 (as measured by ΔG_2) can be made energetically unfavorable through the use of ligands with sufficient steric bulk. Ligands X with five-membered or larger rings proved adequate in this regard in each class of ligands X considered here. The value of ΔG_3 can be raised (or, equivalently, the tendency for η^1-L^1CuXO_2 to decay to L^1CuO_2 + X can be minimized) by increasing the electron-donating capability of the ligand, which the pyridine series of ligands demonstrated. In order to reach endergonic ΔG_3 values, the ancillary ligand must also be capable of engaging in both strong π-backbonding and σ-donation with the copper center as in the case of the carbene ligands. Ancillary ligands X which possess these properties that minimize ΔG_1 and maximize ΔG_2 and ΔG_3, in particular leading to $\Delta G_1 < 0$ and ΔG_2, $\Delta G_3 > 0$, should lead to experimentally isolatable η^1-L^1CuXO_2 species. However, the identity of a ligand X which meets these criteria and is amenable to synthetic methods remains elusive.

Conclusions

Previous work exploring the reactivity of dioxygen with copper(I) complexes supported by β-diketiminate and related biomimetic ligands for the Cu_B site in DβM and PHM has led to the isolation

of η^2 1 : 1 Cu–O_2 adducts. However, the crystal structure of a precatalytic complex of PHM showed dioxygen to be ligated in an end-on fashion to Cu_B. This has provided the impetus to further investigate the η^1-$L^1Cu(THF)O_2$ structure which occurs as an unstable intermediate in the computed mechanism for oxygenation of $L^1Cu(THF)$. To that end, the current work has examined whether an ancillary ligand X other than THF could yield a thermodynamically stable end-on L^1CuXO_2 species. Such a ligand X would lead to exergonic formation of η^1-L^1CuXO_2 from L^1CuX and O_2 as well as inducing isomerization to η^2-L^1CuXO_2 or decay to L^1CuO_2 + X to both be endergonic processes.

A wide range of ancillary ligands X were studied, including phosphines, thiophene, cyclic ethers, acetonitrile, *para*-substituted pyridines, *N*-heterocyclic carbenes, and ligands bearing hydrogen bond donors. This enabled the determination of how strong *versus* weakly coordinating ligands affected O_2 reactivity and the effect of varying the degree of steric bulk around the copper center. Clues as to how variations in the electron-donating capability of the ancillary ligand and the presence of intramolecular hydrogen bonds to the dioxygen moiety would alter the stability of η^1-L^1CuXO_2 were also uncovered.

Properties that an ideal ligand X should possess in order to yield a thermodynamically stable η^1-L^1CuXO_2 species can now be enumerated. Ancillary ligands with strategically sized and positioned steric bulk and/or bearing hydrogen bond donors most favored η^1-L^1CuXO_2 formation from $L^1CuX + O_2$. Isomerization to side-on L^1CuXO_2 was inhibited in the cases where ligands X of sufficient steric bulk (typically, 5-membered rings or larger) were utilized. Lastly, the relative endergonicity for the decay of η^1-L^1CuXO_2 to L^1CuO_2 + X was increased by using more electron-donating ligands and ligands which were excellent simultaneous π-backbonders and σ-donors to copper. Unfortunately, the only ligand studied here which possesses all of these characteristics, thus leading to $\Delta G_1 < 0$ and ΔG_2, $\Delta G_3 > 0$, was the carbene ligand (**16**), which cannot be accessed synthetically, and the search for a feasible ancillary ligand capable of yielding a thermodynamically stable η^1-L^1CuXO_2 species thus remains an open problem.

Acknowledgements

We acknowledge support from the NIH through an NRSA post-doctoral fellowship to B.F.G. and through GM047365 to W.B.T. We also thank the NSF (CHE-0203346 to C.J.C.). D.E.H. acknowledges the Arnold and Mabel Beckman Foundation (Scholar's program award) and the University of Minnesota Department of Chemistry (Gleysteen Scholarship). We thank John T. York for fruitful discussions.

References and notes

1 J. P. Klinman, *Chem. Rev.*, 1996, **96**, 2541.
2 E. I. Solomon, U. M. Sundaram and T. E. Machonkin, *Chem. Rev.*, 1996, **96**, 2563.
3 E. I. Solomon, P. Chen, M. Metz, S. K. Lee and A. E. Palmer, *Angew. Chem., Int. Ed.*, 2001, **40**, 4570.
4 L. C. Stewart and J. P. Klinman, *Annu. Rev. Biochem.*, 1988, **57**, 551.
5 B. A. Eipper, D. A. Stoffers and R. E. Mains, *Annu. Rev. Neurosci.*, 1992, **15**, 57.
6 J. P. Evans, K. Ahn and J. P. Klinman, *J. Biol. Chem.*, 2003, **278**, 49691.
7 P. Chen and E. I. Solomon, *J. Am. Chem. Soc.*, 2004, **126**, 4991.
8 A. T. Bauman, E. T. Yukl, K. Alkevich, A. L. McCormack and N. J. Blackburn, *J. Biol. Chem.*, 2006, **281**, 4190.
9 S. T. Prigge, B. A. Eipper, R. E. Mains and L. M. Amzel, *Science*, 2004, **304**, 864.
10 E. A. Lewis and W. B. Tolman, *Chem. Rev.*, 2004, **104**, 1047.
11 W. B. Tolman, *J. Biol. Inorg. Chem.*, 2006, **11**, 261.
12 K. Fujisawa, M. Tanaka, Y. Morooka and N. Kitajima, *J. Am. Chem. Soc.*, 1994, **116**, 12079.
13 V. V. Smirnov and J. P. Roth, *J. Am. Chem. Soc.*, 2006, **128**, 3683.
14 A. J. Johansson, M. R. A. Blomberg and P. E. M. Siegbahn, *Inorg. Chem.*, 2006, **45**, 1491.
15 M. Schatz, V. Raab, S. P. Foxon, G. Brehm, S. Schneider, M. Reiher, M. C. Holthausen, J. Sundermeyer and S. Schindler, *Angew. Chem., Int. Ed.*, 2004, **43**, 4360.
16 C. Würtele, E. Gaoutchenova, K. Harms, M. C. Holthausen, J. Sundermeyer and S. Schindler, *Angew. Chem., Int. Ed.*, 2006, **45**, 3867.
17 A. Wada, M. Harata, K. Hasegawa, K. Jitsukawa, H. Masuda, M. Mukai, T. Kitagawa and H. Einaga, *Angew. Chem., Int. Ed.*, 1998, **37**, 798.
18 L. E. Cheruzel, M. R. Cecil, S. E. Edison, M. S. Mashuta, M. J. Baldwin and R. M. Buchanan, *Inorg. Chem.*, 2006, **45**, 3191.
19 D. J. E. Spencer, N. W. Aboelella, A. M. Reynolds, P. L. Holland and W. B. Tolman, *J. Am. Chem. Soc.*, 2002, **124**, 2108.
20 N. W. Aboelella, E. A. Lewis, A. M. Reynolds, W. W. Brennessel, C. J. Cramer and W. B. Tolman, *J. Am. Chem. Soc.*, 2002, **124**, 10660.
21 N. W. Aboelella, S. V. Kryatov, B. F. Gherman, W. W. Brennessel, V. G. Young, Jr., R. Sarangi, E. V. Rybak-Akimova, K. O. Hodgson, B. Hedman, E. I. Solomon, C. J. Cramer and W. B. Tolman, *J. Am. Chem. Soc.*, 2004, **126**, 16896.
22 A. M. Reynolds, B. F. Gherman, C. J. Cramer and W. B. Tolman, *Inorg. Chem.*, 2005, **44**, 6989.
23 A. M. Reynolds, E. A. Lewis, N. W. Aboelella and W. B. Tolman, *Chem. Commun.*, 2005, 2014.
24 N. W. Aboelella, B. F. Gherman, L. M. Hill, J. T. York, N. Holm, V. G. Young, Jr., C. J. Cramer and W. B. Tolman, *J. Am. Chem. Soc.*, 2006, **128**, 3345.
25 S. T. Prigge, A. S. Kolhekar, B. A. Eipper, R. E. Mains and L. M. Amzel, *Science*, 1997, **278**, 1300.
26 S. T. Prigge, A. S. Kolhekar, B. A. Eipper, R. E. Mains and L. M. Amzel, *Nat. Struct. Biol.*, 1999, **6**, 976.
27 N. J. Blackburn, S. S. Hasnain, T. M. Pettingill and R. W. Strange, *J. Biol. Chem.*, 1991, **266**, 23120.
28 B. J. Reedy and N. J. Blackburn, *J. Am. Chem. Soc.*, 1994, **116**, 1924.
29 J. S. Boswell, B. J. Reedy, R. Kulathila, D. Merkler and N. J. Blackburn, *Biochemistry*, 1996, **35**, 12241.
30 A. S. Kolhekar, H. T. Keutmann, R. E. Mains, A. S. W. Quon and B. A. Eipper, *Biochemistry*, 1997, **36**, 10901.
31 B. F. Gherman, W. B. Tolman and C. J. Cramer, *J. Comput. Chem.*, 2006, in press.
32 B. F. Gherman, D. E. Heppner, W. B. Tolman and C. J. Cramer, *J. Biol. Inorg. Chem.*, 2006, **11**, 197.
33 N. J. Blackburn, F. C. Rhames, M. Ralle and S. Jaron, *J. Biol. Inorg. Chem.*, 2000, **5**, 341.
34 *Jaguar 5.0*, Schrodinger, LLC, Portland, OR, 2002.
35 J.-M. Ducere, A. Goursot and D. Berthomieu, *J. Phys. Chem. A*, 2005, **109**, 400.
36 B. G. Johnson, P. M. W. Gill and J. A. Pople, *J. Chem. Phys.*, 1993, **98**, 5612.
37 A. D. Becke, *J. Chem. Phys.*, 1993, **98**, 1372.
38 C. T. Lee, W. T. Yang and R. G. Parr, *Phys. Rev. B: Condens. Matter*, 1988, **37**, 785.
39 B. F. Gherman and C. J. Cramer, *Inorg. Chem.*, 2004, **43**, 7281.
40 P. J. Hay and W. R. Wadt, *J. Chem. Phys.*, 1985, **82**, 270.
41 W. R. Wadt and P. J. Hay, *J. Chem. Phys.*, 1985, **82**, 284.
42 P. J. Hay and W. R. Wadt, *J. Chem. Phys.*, 1985, **82**, 299.
43 R. A. Friesner, M.-H. Baik, V. Guallar, B. F. Gherman, M. Wirstam, R. B. Murphy and S. J. Lippard, *Coord. Chem. Rev.*, 2003, **238–239**, 267.
44 M.-H. Baik, M. Newcomb, R. A. Friesner and S. J. Lippard, *Chem. Rev.*, 2003, **103**, 2385.
45 B. Marten, K. Kim, C. Cortis, R. A. Friesner, R. B. Murphy, M. N. Ringnalda, D. Sitkoff and B. Honig, *J. Phys. Chem.*, 1996, **100**, 11775.
46 D. J. Tannor, B. Marten, R. B. Murphy, R. A. Friesner, D. Sitkoff, A. Nicholls, M. N. Ringnalda, W. A. Goddard, III and B. Honig, *J. Am. Chem. Soc.*, 1994, **116**, 11875.

47 C. Carvajal, K. J. Tolle, J. Smid and M. Szwarc, *J. Am. Chem. Soc.*, 1965, **87**, 5548.
48 D. J. Metz and A. Glines, *J. Phys. Chem.*, 1967, **71**, 1158.
49 C. J. Cramer, *Essentials of Computational Chemistry. Theories and Models*, John Wiley & Sons, Ltd. Chichester, UK, 2nd edn, 2004.
50 K. Andersson, P. A. Malmqvist and B. O. Roos, *J. Chem. Phys.*, 1992, **96**, 1218.
51 The study examining the suitability of B3LYP for predicting ligand–Cu(I) bond dissociation energies (ref. 35) did not include phosphorous ligands, such as **8**. It did examine a variety of N, O, and C ligands, providing further evidence for the singularity of the result with **8**.
52 J. T. York, V. G. Young, Jr. and W. B. Tolman, *Inorg. Chem.*, 2006, **45**, 4191.
53 C. Hansch, A. Leo and R. W. Taft, *Chem. Rev.*, 1991, **91**, 165.
54 W. A. Herrmann and C. Kocher, *Angew. Chem., Int. Ed. Engl.*, 1997, **36**, 2162.
55 C. Boehme and G. Frenking, *Organometallics*, 1998, **17**, 5801.
56 X. Hu, I. Castro-Rodriguez, K. Olsen and K. Meyer, *Organometallics*, 2004, **23**, 755.
57 E. D. Glendening, J. K. Badenhoop, A. E. Reed, J. E. Carpenter, J. A. Bohmann, C. M. Morales and F. Weinhold, *NBO 5.0*, Theoretical Chemistry Institute, University of Wisconsin, Madison, WI, 2001 (http://www.chem.wisc.edu/~nbo5).
58 A. E. Reed, L. A. Curtiss and F. Weinhold, *Chem. Rev.*, 1988, **88**, 899.
59 S. Yamaguchi, S. Nagatomo, T. Kitagawa, Y. Funahashi, T. Ozawa, K. Jitsukawa and H. Masuda, *Inorg. Chem.*, 2003, **42**, 6968.
60 K. Jitsukawa, M. Harata, H. Arii, H. Sakurai and H. Masuda, *Inorg. Chim. Acta*, 2001, **324**, 108.
61 N. Kitajima, H. Komatsuzaki, S. Hikichi, M. Osawa and Y. Moro-oka, *J. Am. Chem. Soc.*, 1994, **116**, 11596.
62 A. S. Borovik, *Acc. Chem. Res.*, 2005, **38**, 54.

